Higher Order Dual Lagrange Multiplier Spaces for Mortar Finite Element Discretizations

Bishnu P. Lamichhane* and Barbara I. Wohlmuth*

April 1, 2004

Abstract

Domain decomposition techniques provide a powerful tool for the numerical approximation of partial differential equations. Here, we consider mortar techniques for quadratic finite elements. In particular, we focus on dual Lagrange multiplier spaces. These non-standard Lagrange multiplier spaces yield optimal discretization schemes and a locally supported basis for the associated constrained mortar spaces. As a result, standard efficient iterative solvers as multigrid methods can be easily adapted to the nonconforming situation. We construct locally supported and continuous dual basis functions for quadratic finite elements starting from the discontinuous quadratic dual basis functions for the Lagrange multiplier space. In particular, we compare different dual Lagrange multiplier spaces and piecewise linear and quadratic finite elements. The optimality of the associated mortar method is shown. Numerical results illustrate the performance of our approach.

Key words. mortar finite elements, Lagrange multiplier, dual space, domain decomposition, non-matching triangulation
AMS subject classification. 65N30, 65N55

1 Introduction

Nonconforming domain decomposition techniques provide a more flexible approach than standard conforming formulations. They are of special interest for time dependent problems, rotating geometries, diffusion coefficients with jumps, problems with local anisotropies, corner singularities, and when different terms dominate in different regions of the simulation domain. Very often heterogeneous problems can be decomposed into homogeneous subproblems for which efficient discretization techniques are available. To obtain a stable and optimal discretization scheme for the global problem, the information transfer and the communication between the subdomains are of crucial importance. We present our approach within the framework of mortar methods [BMP93, BMP94]. Originally introduced

*Institute of Applied Analysis and Numerical Simulation, University of Stuttgart, Pfaffenwaldring 57, D–70 569 Stuttgart, Germany, lamichhane@mathematik.uni-stuttgart.de, wohlmuth@mathematik.uni-stuttgart.de

as a domain decomposition method for the coupling of spectral elements, these techniques are nowadays used in a large class of nonconforming situations. Thus, the coupling of different physical models, discretization schemes, or non-matching triangulations along interior interfaces of the domain can be analyzed by mortar methods. In this paper, we concentrate on mortar methods for quadratic finite elements. Higher order mortar methods are considered in different recent papers. Uniform hp convergence results for the mortar method are established in [SS00, SS98], and in [OW01] discontinuous higher order Lagrange multiplier spaces are introduced. The generalization of the low order mortar method to 3D case can be found in [BM97, BD98, KLPV01]. A different nonconforming technique is based on the Nitsche method, see [Ste98, BHS01, HN01].
The paper is organized as follows: In the rest of this section, we briefly recall the mortar finite element method. We focus on so-called dual Lagrange multiplier spaces. In Section 2, we construct new dual Lagrange multipliers being locally supported and continuous. We start with the discontinuous dual Lagrange multiplier introduced in [Woh01] and add local correction terms. It can be shown that we obtain the same qualitative a priori estimates for the discretization errors. In Section 3, we give a negative result for dual Lagrange multiplier space in 3D for simplicial triangulations. Finally in Section 4, we present numerical results for different dual Lagrange multiplier spaces illustrating the performance of the nonconforming approach. Numerical results are given for different types of domain decompositions in 2D. In particular, we compare the discretization error in the L^2-norm, the energy norm and in a weighted L^2-norm for quadratic and linear mortar finite elements. Additionally, we illustrate the influence of different Lagrange multiplier spaces on the accuracy.

We consider the following elliptic second order boundary value problem

$$\begin{aligned} -\mathrm{div}(a\nabla u) + bu &= f \quad \text{in } \Omega \ , \\ u &= 0 \quad \text{on } \partial\Omega \ . \end{aligned}$$

Here, $0 < a_0 \leq a \in L^\infty(\Omega)$, $f \in L^2(\Omega)$, $0 \leq b \in L^\infty(\Omega)$, and $\Omega \subset \mathrm{R}^2$, is a bounded polygonal domain. Let Ω be decomposed into K non-overlapping polygonal subdomains Ω_k such that $\overline{\Omega} = \bigcup_{k=1}^{K} \overline{\Omega}_k$. We restrict ourselves to the geometrically conforming situation where the intersection between the boundaries of any two different subdomains $\partial\Omega_l \cap \partial\Omega_k$, $k \neq l$, is either empty, a vertex or a common edge. We define on each subdomain a simplicial or quadrilateral triangulation $\mathcal{T}_{k;h_k}$, the meshsize of which is bounded by h_k. The discrete space of conforming piecewise quadratic or biquadratic finite elements on Ω_k associated with $\mathcal{T}_{k;h_k}$, which satisfies homogeneous Dirichlet boundary conditions on $\partial\Omega \cap \partial\Omega_k$, is denoted by X_{h_k}. Then, the mortar method is characterized by the introduction of a discrete Lagrange multiplier space $M_{h_m}(\gamma_m)$ on the interfaces γ_m, $1 \leq m \leq M$, of the decomposition. For each interface, there exists a couple $1 \leq l(m) < k(m) \leq K$ such that $\overline{\gamma}_m = \partial\Omega_{l(m)} \cap \partial\Omega_{k(m)}$. Moreover, each interface γ_m is associated with a one-dimensional mesh $\mathcal{S}_{m;h_m}$, inherited from either $\mathcal{T}_{k(m);h_{k(m)}}$ or $\mathcal{T}_{l(m);h_{l(m)}}$. The choice is arbitrary but should be fixed. In general, these meshes do not coincide. The elements of $\mathcal{S}_{m;h_m}$ are boundary edges of either $\mathcal{T}_{l(m);h_{l(m)}}$ or $\mathcal{T}_{k(m);h_{k(m)}}$. The subdomain from which the interface inherits its triangulation is called slave or non-mortar side, the opposite one master or mortar side.

To obtain the mortar approximation u_h, as a solution of a discrete variational problem, there are two main approaches. The first one has been introduced in [BMP93, BMP94] and gives rise to a positive definite nonconforming variational problem. It is defined on a subspace V_h of the product space $X_h := \{v \in L^2(\Omega) \mid \ v_{|\Omega_k} \in X_{h_k}, 1 \leq k \leq K\}$. The elements of V_h satisfy a weak continuity condition across the interfaces. The constrained finite element

space V_h is given by

$$V_h := \{ v \in X_h \mid \int_{\gamma_m} [v] \mu \, d\sigma = 0, \, \mu \in M_{h_m}(\gamma_m), \, 1 \leq m \leq M \} \ .$$

Then, the nonconforming formulation of the mortar method can be given in terms of the constrained space V_h: Find $u_h \in V_h$ such that

$$a(u_h, v_h) = (f, v_h)_0, \quad v_h \in V_h \ . \tag{1.1}$$

We refer to [BMP93, BMP94] for the original introduction of the constrained space. Here, the bilinear form $a(\cdot, \cdot)$ is defined as

$$a(v, w) := \sum_{k=1}^{K} \int_{\Omega_k} a \nabla v \cdot \nabla w + bv \, w \, dx, \quad v, w \in \prod_{k=1}^{K} H^1(\Omega_k) \ .$$

The second approach is based on an equivalent saddle point formulation, see [Bel99]. It is obvious that the quality of the nonconforming approach (1.1) and the properties of V_h depend on the discrete Lagrange multiplier space $M_h := \prod_{m=1}^{M} M_{h_m}(\gamma_m)$. The mortar method is characterized by the fact that a weak matching condition is imposed on the interface in terms of the L^2-orthogonality of the jumps of the solution

$$\int_{\gamma_m} [v_h] \ \mu_i \, d\sigma = 0, \quad 1 \leq i \leq n_m, \ 1 \leq m \leq M \ , \tag{1.2}$$

where $n_m := \dim M_{h_m}(\gamma_m)$ and $\{\mu_i\}_{1 \leq i \leq n_m}$ defines a basis of $M_{h_m}(\gamma_m)$. To obtain a discretization scheme of optimal order, the Lagrange multiplier space has to be chosen carefully. It has to be large enough to obtain an optimal consistency error. On the other hand, it has to be small enough to get an optimal best approximation error and a uniform discrete inf-sup condition. A natural and efficient choice for the construction of good Lagrange multiplier spaces is to define the nodal Lagrange multiplier basis function locally and to associate them with the interior nodes of the slave side. In the following, we restrict ourselves to these situations. Now, we group the degrees of freedom of X_h associated with the interface γ_m into two groups $u_{|\gamma_m} := (u_s, u_m)$. Here, u_s consists of all nodal values of u at the interior nodes of γ_m on the slave side and u_m represents all nodal values of u at the interior nodes of the master side and all nodal values at the nodes on the boundary of the interface γ_m, see Figure 1.

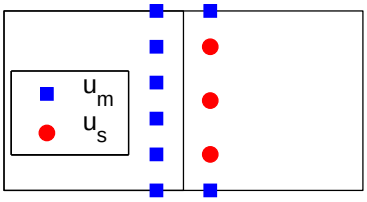

Figure 1: The two groups of nodes on the interface

Then (1.2) can be written in its algebraic form as

$$M_s u_s = M_m u_m \ , \tag{1.3}$$

where the entries of the mass matrices are given by $m_{ij} := \int_{\gamma_m} \phi_j \ \mu_i \, d\sigma$, and ϕ_j corresponds to the different nodal basis functions on the slave and master side. The mass matrices are sparse due to the local structure of the supports of the involved basis functions. Formally, we can obtain the values on the slave side as $u_s = M_s^{-1} M_m u_m$. We note that M_s is a square matrix whereas M_m is a rectangular matrix. In general, the inverse of the mass matrix M_s is dense, and thus the values on the slave side depend globally on the values on the master side. If M_s in (1.3) is a diagonal matrix, then the values of u_s depend locally on the values of the master side. This observation motivates our interest in dual Lagrange multiplier spaces. Let us denote the trace space of finite element functions on the slave side having zero boundary conditions on $\partial\gamma_m$ by $W_{0;h}(\gamma_m)$. The associated nodal basis functions are called $\varphi_i, 1 \leq i \leq n_m$, where $n_m := \dim(W_{0;h}(\gamma_m))$.

Definition 1 *The Lagrange multiplier basis functions $\{\mu_i\}_{1\leq i\leq n_m}$ of $M_{h_m}(\gamma_m)$ and the nodal basis functions $\{\varphi_i\}_{1\leq i\leq n_m}$ of the trace space $W_{0,h}(\gamma_m)$ are called biorthogonal and the Lagrange multiplier space dual if and only if*

$$\int_{\gamma_m} \mu_i \ \varphi_j \, d\sigma = c_i \delta_{ij} \int_{\gamma_m} \varphi_j \, d\sigma \ , \quad 1 \leq i, j \leq n_m,$$

where $c_i \neq 0$. Without loss of generality, we can assume that $c_i = 1$.

2 Quadratic Dual Lagrange Multiplier Spaces

Dual Lagrange multiplier spaces have been considered in [Woh00] for low order finite elements. Recently they have been generalized to higher order finite elements in [OW01]. In [OW01], we cannot satisfy $\mathrm{supp}\varphi_i = \mathrm{supp}\mu_i$ and the support of μ_i is larger. Here, we consider some examples of dual Lagrange multiplier spaces for quadratic finite elements with $\mathrm{supp}\varphi_i = \mathrm{supp}\mu_i$. Starting with the piecewise quadratic biorthogonal basis functions presented in [Woh01], we construct locally supported continuous biorthogonal basis functions. We denote by $\hat{\varphi}_0, \hat{\varphi}_1$ and $\hat{\varphi}_2$ the quadratic nodal finite element basis functions on the reference element [0,1] in one dimension, where $\hat{\varphi}_0$ is the basis function corresponding to the midpoint of the reference element and $\hat{\varphi}_1$ and $\hat{\varphi}_2$ are the basis functions corresponding to the left and the right vertices, respectively. Now, the quadratic dual Lagrange multiplier basis functions in the reference element are defined by

$$\lambda_0 \ = \ \frac{5}{2}\hat{\varphi}_0 \ - \ 1, \quad \lambda_1 \ = \ \hat{\varphi}_1 \ - \ \frac{3}{4}\hat{\varphi}_0 \ + \ \frac{1}{2}, \quad \lambda_2 \ = \ \hat{\varphi}_2 \ - \ \frac{3}{4}\hat{\varphi}_0 \ + \ \frac{1}{2}. \quad (2.4)$$

Then it is easy to verify

$$\int_0^1 \lambda_i \hat{\varphi}_j \, d\sigma = \delta_{ij} \int_0^1 \hat{\varphi}_j \, d\sigma, \quad 0 \leq i, j \leq 2.$$

The approximation property of the Lagrange multiplier for quadratic finite elements requires that the constants and the linear functions are contained in the Lagrange multiplier space $M_h(\gamma_m)$. To satisfy these conditions, the Lagrange multipliers have to be modified near the crosspoints. If $t = 0$ is the crosspoint, we use the following definition for the Lagrange multipliers on the reference edge

$$\lambda_0(t) = -2t + 2, \quad \lambda_1(t) = 2t - 1 \quad (2.5)$$

and if $t = 1$ is the crosspoint

$$\lambda_0(t) = 2t, \quad \lambda_1(t) = 1 - 2t. \tag{2.6}$$

We note that λ_2 does not exist if $t = 0$ or $t = 1$ is a crosspoint. The global basis functions μ_i are obtained by using an affine mapping and glueing the local ones at the vertices together, see [Woh01]. The two pictures in the left of the Figure 2 illustrate the interior Lagrange multipliers. The left one is associated with the midpoint of an edge and the right one with a vertex. In the two pictures on the right, the situation of a left crosspoint is shown. The left one gives the Lagrange multiplier associated with the interior vertex and the right one shows the one associated with the midpoint of the edge.

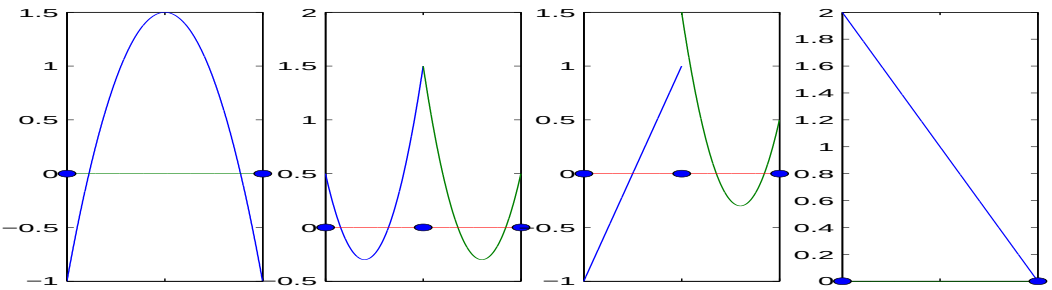

Figure 2: Interior dual basis functions (left 1 and 2) and modification at a left crosspoint (right 1 and 2), discontinuous case

Although these dual basis functions are locally supported and optimal a priori bounds hold, the use of discontinuous Lagrange multiplier spaces can be disadvantageous if some inexact quadrature formulas are used. To assemble the mass matrix M_m, we have to compute the integral of the product of two discrete functions defined on two completely different meshes. The discontinuities of the Lagrange multipliers which are living on the slave side will lead to a considerable loss of accuracy in the integral computation if the quadrature nodes are not adapted to the discontinuities. Since we have independent meshes on the slave and the master side, the discontinuities of the Lagrange multiplier basis functions are not captured by quadrature points based on the master side. Therefore, it might be better to work with continuous Lagrange multiplier spaces. Now, the idea is to modify locally the piecewise quadratic dual basis functions by adding some local correction functions g, h_1 and h_2, i.e., $\hat{\lambda}_0 = \lambda_0 + g$, $\hat{\lambda}_1 = \lambda_1 + h_1$ and $\hat{\lambda}_2 = \lambda_2 + h_2$. The associated global Lagrange multiplier basis functions $\hat{\mu}_i$ have to satisfy

[P0] $\hat{\mu}_i$ is continuous

[P1] $\operatorname{supp} \hat{\mu}_i = \operatorname{supp} \mu_i$

[P2] $\sum_{i=1}^{n_m} \hat{\mu}_i = 1$

[P3] $\int_{\gamma_m} \hat{\mu}_i \, \varphi_j \, d\sigma = \delta_{ij} \int_{\gamma_m} \varphi_j \, d\sigma$

[P4] $\|\hat{\mu}_i\|_0 \equiv \|\varphi_i\|_0$ and $|\hat{\mu}_i|_1 \equiv |\varphi_i|_1$.

To do so, we start with the piecewise quadratic dual Lagrange multiplier basis functions on the reference element. Let λ_0, λ_1 and λ_2 be the quadratic dual basis functions corresponding to the midpoint, left and right vertices of the reference element, we have to find a function g for λ_0 such that the conditions

[g0] $g(1) + \lambda_0(1) = 0,$

[g1] $g(0) + \lambda_0(0) = 0$ and

[g2] $\int_0^1 g\, p\, dt = 0$ for all quadratic functions $p \in P_2([0,1])$

are satisfied. Similarly, we have to find functions h_1 for λ_1 and h_2 for λ_2 such that

[h0] $h_1(1) + \lambda_1(1) = 0, \quad h_2(1) + \lambda_2(1) = 1$

[h1] $h_1(0) + \lambda_1(0) = 1, \quad h_2(0) + \lambda_2(0) = 0$ and

[h2] $\int_0^1 h_i\, p\, dt = 0$ for all quadratic functions $p \in P_2([0,1])$, $i = 1, 2,$

are satisfied. Furthermore, we require that $h_1 + h_2 + g = 0$ on $[0,1]$ and that $g, h_1, h_2 \in H^1([0,1])$. Then the modified Lagrange multipliers $\hat{\mu}_i$ are obtained by an affine mapping from the ones on the reference edge. We note that we do not modify the definition of a Lagrange multiplier restricted to an edge having one crosspoint.

Lemma 2 *The modified basis functions $\hat{\mu}_i$ satisfy the properties [P0]–[P4].*

The properties [P0]–[P4] follow by construction. Of course, there are many choices for g, h_1 and h_2. Regarding $[h0]$ and $[h1]$, we can choose $h_1 = h_2 = h$. In the following, we discuss different possibilities for h and g. One possibility is to consider the case where g and h are polynomials of minimal degree satisfying the given conditions. Another possibility is to define g and h as piecewise quadratic functions on $[0,1]$. Following the first possibility, we get unique quartic polynomials g and h on $[0,1]$ such that the modified Lagrange multipliers have all the properties listed above. The polynomial g on $[0,1]$ is explicitly given by

$$g(t) := 70t^4 - 140t^3 + 90t^2 - 20t + 1 \quad \text{and} \quad h := -g/2. \tag{2.7}$$

The modified Lagrange multipliers are shown in Figure 3, and the correction g is given in the left picture of Figure 4. The conditions $[g2]$ and $[h2]$ ensure the biorthogonality, and it can be easily seen that the correction g is reflection invariant on [0,1], i.e., $g(t) = g(1-t)$. The maximum value of the nodal Lagrange multiplier basis function associated with the midpoint is 1.875.

In the following examples, we consider piecewise quadratic corrections in $[0,1]$ satisfying the properties $[g0] - [g2]$ and $[h0] - [h2]$. We have to decompose the unit interval at least into two subintervals. In the case of two subintervals, the correction g is uniquely defined. If we use more than two subintervals, we can impose additional conditions on g. Using $[0, 1/2)$ and $[1/2, 1]$, we find

$$g(t) := \begin{cases} 30t^2 - 14t + 1, & 0 \le t < \frac{1}{2}\,, \\ 30t^2 - 46t + 17, & \frac{1}{2} \le t \le 1\,, \end{cases} \quad \text{and} \quad h := -g/2. \tag{2.8}$$

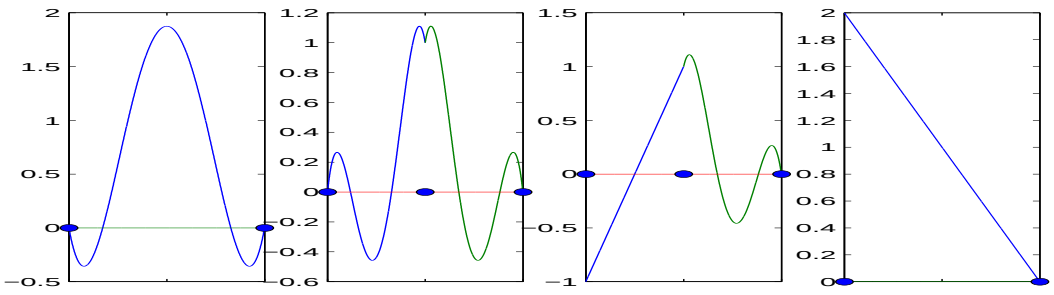

Figure 3: Interior dual basis functions (left 1 and 2) and modification at a left crosspoint (right 1 and 2), quartic correction

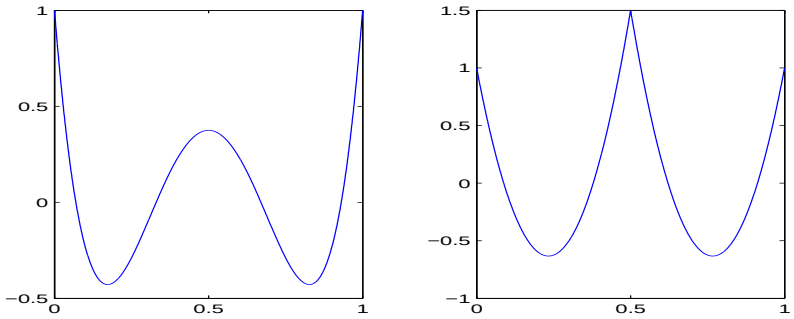

Figure 4: The quartic correction g (left) and the piecewise quadratic one (right)

The correction g is given in the right of Figure 4, and the associated dual basis functions are shown in Figure 5.

Another possibility is to decompose the unit interval $[0,1]$ into three subintervals and consider piecewise linear polynomials in two subintervals and a piecewise quadratic in the third one. Then, we get a unique correction function g. If we choose piecewise linear functions in the left and right subintervals $[0,1/3)$ and $[2/3,1]$ and a quadratic polynomial in the middle subinterval $[1/3,2/3)$, g is defined by

$$g(t) := \begin{cases} 1 - \frac{189}{22}\ t, & 0 \le t < \frac{1}{3}\ , \\ -\frac{1620}{11}t^2 + \frac{1620}{11}t - \frac{761}{22}, & \frac{1}{3} \le t < \frac{2}{3}\ , \\ \frac{189}{22}t - \frac{167}{22}, & \frac{2}{3} \le t \le 1, \end{cases} \qquad \text{and} \quad h := -g/2.$$

The correction function g is shown in the left of Figure 7 and the associated basis function in Figure 6.

Although there are many possibilities to construct continuous Lagrange multipliers, the numerical experiments show that the Lagrange multipliers with smaller maximum value on the reference element give better results. To get a symmetric Lagrange multiplier which has a smaller maximum, we consider another case with piecewise quadratic functions in $[0,1/3)$ and $[2/3,1)$ and being constant in the middle interval $[1/3,2/3)$. Then, we get a unique g

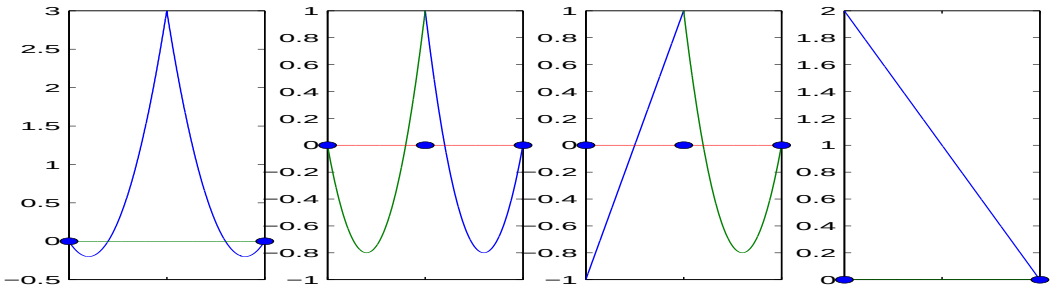

Figure 5: Interior dual basis functions (left 1 and 2) and modification at a left crosspoint (right 1 and 2), piecewise quadratic correction

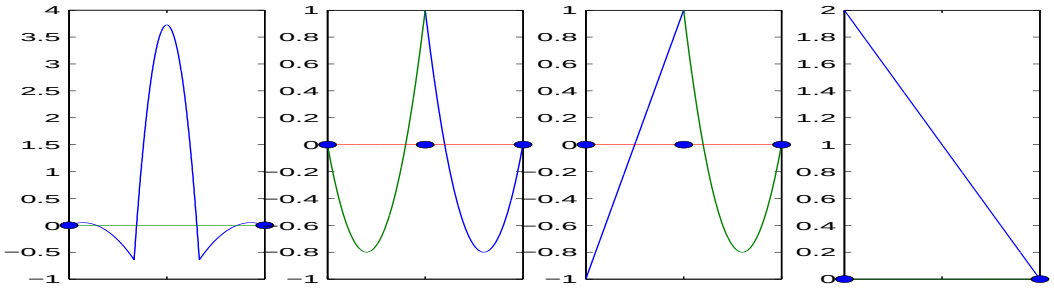

Figure 6: Interior dual basis functions (left 1 and 2) and modification at a left crosspoint (right 1 and 2), piecewise linear and quadratic correction

defined by

$$g(t) := \begin{cases} \frac{810}{19}\,t^2 - \frac{621}{38}\,t + 1, & 0 \le t < \frac{1}{3}\ , \\ \frac{11}{38}, & \frac{1}{3} \le t < \frac{2}{3}\ , \\ \frac{810}{19}\,t^2 - \frac{2619}{38}\,t + \frac{1037}{38}, & \frac{2}{3} \le t \le 1\ , \end{cases} \qquad \text{and} \quad h := -g/2. \tag{2.9}$$

The correction function g is given in the right picture of Figure 7, and the associated dual basis functions are shown in Figure 8. We note that if we want to minimize the maximum value of the Lagrange multiplier on the reference element corresponding to the midpoint of the edge by relaxing the condition of symmetry, it is possible to find another Lagrange multiplier with a smaller maximum value. But the difference is very small.

Remark 3 *The Lagrange multiplier space spanned by the discontinuous quadratic functions given by* (2.4), (2.5) *and* (2.6) *will be denoted by* M_h^d, *and the Lagrange multiplier spaces spanned by the continuous functions which are corrected by* g *and* h *given in* (2.7), (2.8) *and* (2.9) *will be denoted by* M_h^q, M_h^b *and* M_h^c, *respectively. Similarly we will denote by* M_h^l *the dual Lagrange multiplier space for linear finite elements spanned by piecewise linear functions.*

The optimality of the discretization scheme depends on the verification of the properties (Sa)-(Sd) of the Lagrange multiplier space presented in [Woh01]. In the case of dual Lagrange

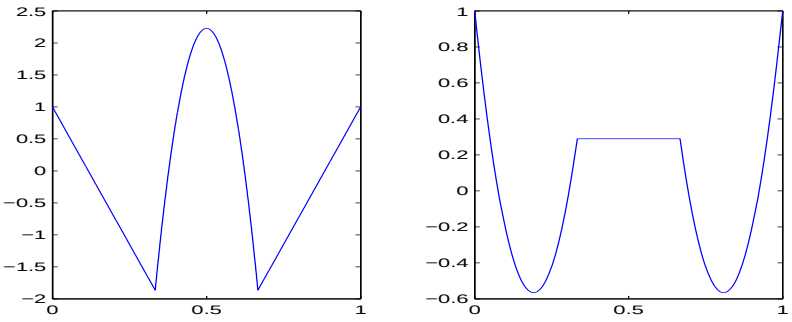

Figure 7: The piecewise linear and quadratic correction g (left) and piecewise constant and quadratic one (right)

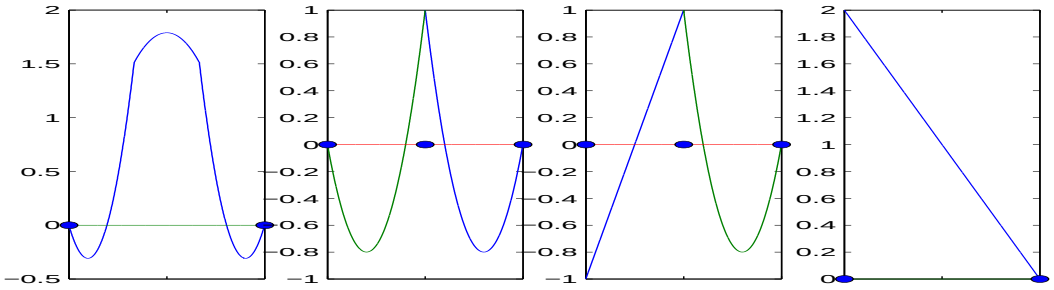

Figure 8: Interior dual basis functions (left 1 and 2) and modification at a left crosspoint (right 1 and 2), piecewise quadratic and constant correction

multiplier spaces this can be easily done by verifying that the constants and the linear functions are contained in the Lagrange multiplier spaces. In particular, we find for all our spaces

$$\phi_p^l = \mu_p + \frac{1}{2}(\mu_{e1} + \mu_{e2}),$$

where ϕ_p^l is the hat function at the vertex p, and μ_p is the Lagrange multiplier basis function corresponding to the same vertex, and μ_{e1} and μ_{e2} are the basis functions associated with the midpoints of the two adjacent edges. We measure the error in the Lagrange multiplier μ in a broken dual norm defined by

$$\|\mu - \mu_h\|_M = \sum_{m=1}^{M} \|\mu - \mu_h\|_{-1/2,\gamma_m}$$

where $\|.\|_{-1/2,\gamma_m}$ is the dual norm of $H_{00}^{1/2}(\gamma_m)$ and $\mu = a\frac{\partial u}{\partial n}$.

Lemma 4 *Under the assumption that the weak solution is smooth enough, we obtain the following a priori estimates for the discretization error*

$$\frac{1}{h}\|u - u_h\|_0 + \|u - u_h\|_1 + \|\mu - \mu_h\|_M = \mathcal{O}(h^2).$$

3 Dual Lagrange Multiplier Spaces in 3D

In this section, we consider the extension to the 3D case. Using hexahedral triangulations and finite element spaces having a tensor product structure, we can directly apply the 2D results, and define the Lagrange multipliers as tensor product. However, the situation is not as simple for simplicial triangulations. To obtain optimal a priori error estimates, it is sufficient that the linear functions are contained in $M_h(\gamma_m)$. We denote by $W_h^1(\gamma_m)$ the finite element space of piecewise linear hat functions. In all our 2D examples, even the hat functions are elements of $M_h(\gamma_m)$. Unfortunately, this does not hold in 3D for simplicial triangulations. Let us assume that the nodal basis functions of our dual Lagrange multiplier space satisfy $\text{supp}\varphi_i = \text{supp}\mu_i$, where φ_i are the standard nodal quadratic finite element basis functions.

Lemma 5 *Under the above assumption, there exists no dual Lagrange multiplier space $M_h(\gamma_m)$ such that $W_h^1(\gamma_m) \subset M_h(\gamma_m)$.*

Proof: The proof is carried out by contradiction. Let us assume that

$$\sum_i \alpha_i \mu_i = \phi_p^l, \tag{3.10}$$

where ϕ_p^l is the hat function associated with the interior vertex p, see Figure 9.

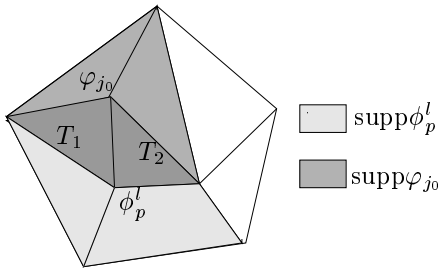

Figure 9: 2D interface of 3D simplicial triangulation

Because of the duality, the functions μ_i are biorthogonal to the finite element basis functions φ_j on the slave side of the interface. Hence, after multiplying (3.10) by some finite element basis function φ_j and integrating over the interface γ_m, we get

$$\alpha_j = \frac{\int_{\gamma_m} \varphi_j \phi_p^l \, d\sigma}{\int_{\gamma_m} \varphi_j \, d\sigma}.$$

Let j_0 be another interior vertex such that j_0 and p share one edge, see Figure 9. Then, we can write

$$\int_{\gamma_m} \varphi_{j_0} \phi_p^l \, d\sigma = \int_{T_1} \varphi_{j_0} \phi_p^l \, d\sigma + \int_{T_2} \varphi_{j_0} \phi_p^l \, d\sigma = -(|T_1| + |T_2|)/60$$

and thus $\alpha_{j_0} \neq 0$. Since the basis functions μ_i are locally linearly independent, we obtain that $\text{supp} \sum_j \alpha_j \mu_j \supseteq \text{supp}\mu_{j_0}$. By construction, we find $\text{supp}\mu_{j_0} \subsetneq \text{supp}\phi_p^l$. ■

4 Numerical Results

Here, we present some numerical examples which illustrate the flexibility and efficiency of the mortar finite element method with dual Lagrange multipliers. Our numerical realization is based on the finite element toolbox ug, [BBJ+97]. In the first subsection, we present the comparison of linear and piecewise quadratic mortar finite elements. In the second subsection, we compare the performance of the discontinuous quadratic dual Lagrange multiplier space M_h^d with the continuous dual Lagrange multiplier spaces M_h^q, M_h^b and M_h^c.

4.1 Comparison of Linear and Quadratic Mortar Finite Elements

In this subsection, we present the numerical results in two dimensions for various types of domain decompositions comparing the discretization errors for linear and quadratic mortar finite elements. Here, we use a mesh dependent L^2-norm for the Lagrange multiplier

$$\|\mu - \mu_h\|_h^2 := \sum_{m=1}^{M} \sum_{e \in \mathcal{S}_{m;h_m}} h_e \|\mu - \mu_h\|_{0;e}^2 \ ,$$

where h_e is the length of the edge e on the slave side.

In our first example, we consider a decomposition of a square $\Omega = (0,1) \times (0,1)$ into two subdomains Ω_1 and Ω_2, where Ω_1 is a closed polygonal non-convex subdomain joining the points $(0,0), (1,0), (1/2,1/2), (1,1)$ and $(0,1)$ and Ω_2 is a triangle with the vertices $(1,0), (1,1)$ and $(1/2,1/2)$. Figure 10 shows the decomposition into two subdomains, the non-matching initial triangulation and the isolines of the solution. We have two interfaces and three crosspoints. The master sides are defined to be on the non-convex subdomain, and the slave subdomain is the triangle. Here, we solve the Poisson equation $-\Delta u = f$ in Ω, where the right hand side and the Dirichlet boundary conditions are determined by choosing the exact solution $u(x,y) = xy(x-1)(y-1)$. We denote the mortar solution for linear finite elements by u_h^l and the one for quadratic finite elements using the space M_h^d by u_h^d.

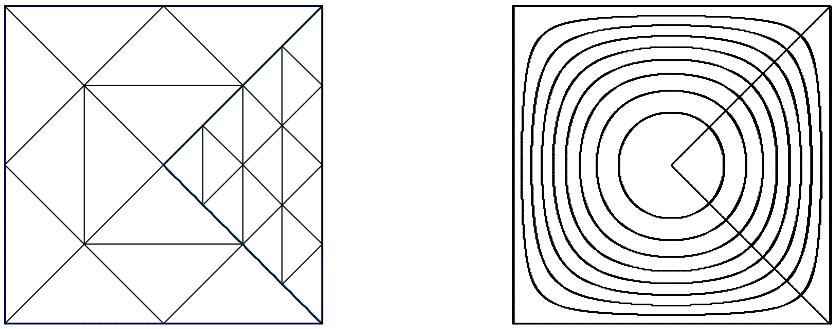

Figure 10: Decomposition into two subdomains and initial triangulation (left) and isolines of the solution (right), (Example 1)

Figure 11 shows the discretization errors in the L^2-, H^1- and Lagrange multiplier norm versus the number of elements. The asymptotic rates confirm the theory of linear and quadratic mortar finite element methods. We find that the energy error is of order h and h^2

whereas the error in the L^2-norm is of order h^2 and h^3 for the linear and the quadratic case, respectively. The correct order can be observed from the beginning. In the right picture of Figure 11, the error in the Lagrange multiplier at the interface is given.

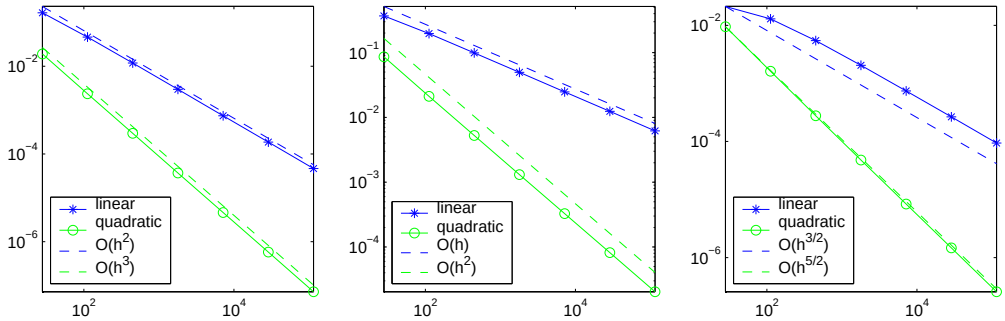

Figure 11: Error plot versus number of elements, L^2-norm (left), H^1-norm (middle), weighted Lagrange multiplier norm (right), (Example 1)

Although from the theoretical point of view, we can expect that the error is of order h in the linear case and of order h^2 in the quadratic case, the numerical results show that the convergence is of order $h^{3/2}$ for the linear case and of order $h^{5/2}$ for the quadratic case. The observed superconvergence behavior can be explained in the same way as in [Woh02]. The a priori analysis of the Lagrange multiplier error consists of two terms. The first one is the best approximation property which is of order $h^{3/2}$ in the linear case and of order $h^{5/2}$ in the quadratic case, whereas the second one involves the energy norm which can only be expected to be of order h in the linear case and of h^2 in the quadratic case. However, it is sufficient to take into account the energy error in a small strip of width h on the slave side. If we assume that the error in the energy norm is equidistributed, we find that the error in the strip is bounded by $Ch^{1/2}$ times the error in the slave subdomain. As a consequence, better asymptotic results for the Lagrange multiplier can be observed, see the right picture of Figure 11.

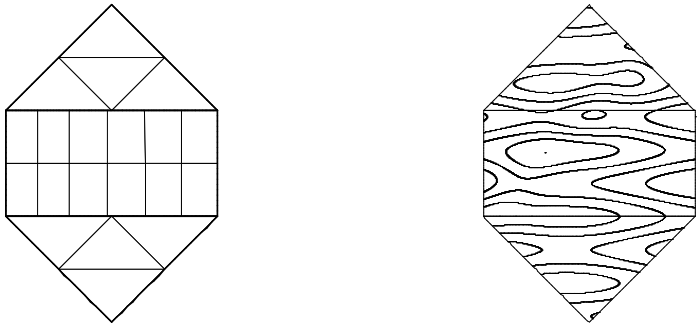

Figure 12: Decomposition into three subdomains and initial triangulation (left) and isolines of the solution (right), (Example 2)

In our next example, we consider a polygonal domain Ω with vertices $(0,0)$, $(1,-1)$, $(2,0)$, $(2,1)$, $(1,2)$ and $(0,1)$ which is decomposed into three subdomains, see Figure 12. Here Ω_1 is $(0,2) \times (0,1)$ whereas Ω_2 is the triangle with vertices $(0,0), (1,-1)$ and $(1,0)$, and Ω_3

is also a triangle joining the points $(0,1),(1,2)$ and $(2,1)$. The subdomain Ω_1 is the slave subdomain and Ω_2 and Ω_3 are master subdomains. We have two interior interfaces and four crosspoints. We compute the numerical solution of the Poisson equation $-\Delta u = f$, where the right hand side and the Dirichlet boundary conditions are determined by choosing the exact solution $u(x,y) = \exp(-10(x-y)^2)\cos(x^2+2y^2) + \sin(2x) + \cos(10y)$. Figure 12 shows the initial non-matching triangulation and the isolines of the solution. We note that the triangulation on Ω_1 is non-symmetric with respect to the x-axis.

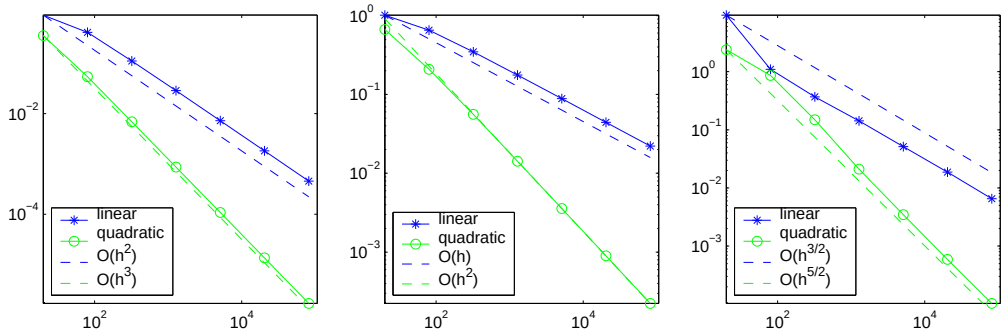

Figure 13: Error plot versus number of elements, L^2-norm (left), H^1-norm (middle), weighted Lagrange multiplier norm (right), (Example 2)

The discretization errors for the different norms versus the number of elements are shown in Figure 13. As in the first example, we observe the same asymptotic rates and superconvergence in the weighted Lagrange multiplier norm. The numerical results confirm the theory.

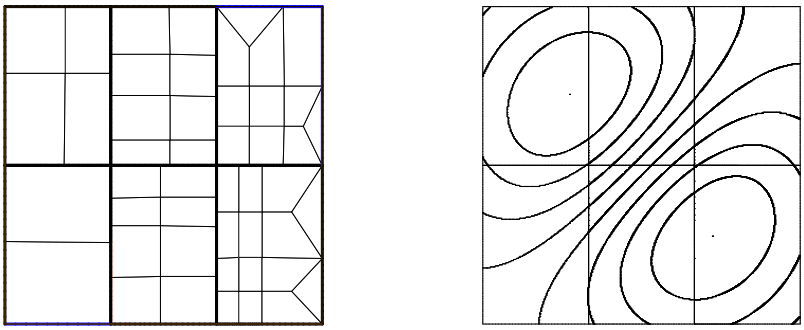

Figure 14: Decomposition into six subdomains and initial triangulation (left) and isolines of the solution (right), (Example 3)

In our last example, we consider the decomposition of $\Omega = (0,1)\times(0,1)$ into six subdomains defined by $\Omega_{ij} := ((i-1)/3, i/3)\times((j-1)/2, j/2), 1 \le i \le 3, 1 \le j \le 2$, and the triangulations do not match at the interfaces. We have two interior crosspoints and seven interfaces. The meshes at the interfaces are non-matching and the master sides are chosen randomly. The right hand side f and the Dirichlet boundary conditions of $-\Delta u = f$ are chosen such that the exact solution is given by $u(x,y) = (x-y)\exp(-5(x-0.5)^2 - 5(y-0.5)^2)$. Figure 14 shows the decomposition into subdomains, initial non-matching triangulation and the isolines of the solution. The numerical results for the discretization errors in the L^2-, H^1- and the weighted Lagrange multiplier norm are given in Figure 15. A good agreement

between numerical and theoretical results can be observed.

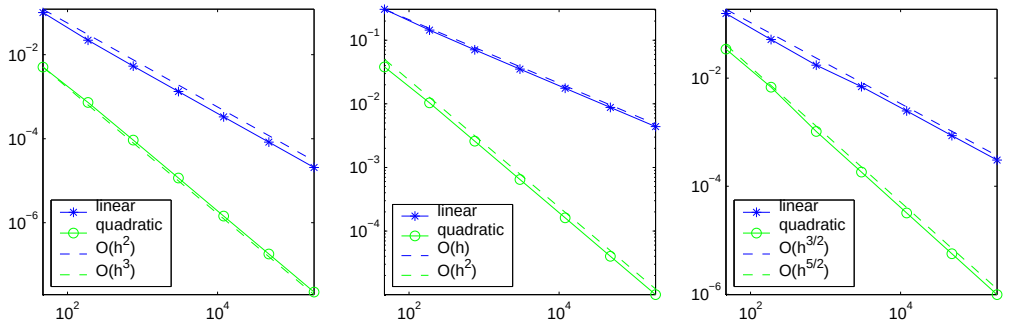

Figure 15: Error plot versus number of elements, L^2-norm (left), H^1-norm (middle), weighted Lagrange multiplier norm (right), (Example 3)

4.2 Comparison of Discontinuous and Continuous Lagrange Multipliers

In this subsection, we compare the performance of our new continuous dual Lagrange multiplier spaces M_h^q, M_h^b and M_h^c with the piecewise quadratic but discontinuous dual Lagrange multiplier space M_h^d. Due to the fact that the continuous quartic Lagrange multiplier is locally a fourth order polynomial, we have to use a higher order quadrature formula to compute the integral in the mass matrix and the weighted error norm for the Lagrange multiplier. We denote by u_h^d, u_h^q, u_h^b and u_h^c the mortar finite element solutions associated with the different Lagrange multiplier spaces M_h^d, M_h^q, M_h^b and M_h^c, respectively. We use the same test examples as before. Tables 1-3 show the numerical results for the three different examples and for the four different choices of Lagrange multipliers. The discretization errors in the L^2- and H^1-norm for the weak solution u are exactly the same for the first example, and in the two other examples the differences are extremely small. Therefore, we do not give the tables. A small difference can be observed only in the error in the Lagrange multiplier. If we compare the other Lagrange multiplier spaces with the discontinuous Lagrange multiplier space, we observe that the continuous quartic Lagrange multiplier space yields an error of about 3 % higher in the first level and in the final level the difference is about 5 % whereas the error for the broken-quadratic Lagrange multiplier space is about 24 % higher in the first level which goes up to 58 % in the final refinement level. The error for the broken-constant Lagrange multiplier space is about 0.3 % less in the first level and around 2 % in the final refinement level. The bigger error in the Lagrange multiplier norm for M_h^b is due to the fact that the maximum value of the nodal basis function is higher compared to the other Lagrange multiplier basis functions. In fact, the maximum value of nodal basis function from M_h^b corresponding to the midpoint of the edge is 3 whereas the maximum value of the discontinuous Lagrange multiplier at this node is 1.5. The broken-constant Lagrange multiplier has a maximum value of 1.8.

Table 1: Discretization errors in the weighted Lagrange multiplier norm, (Example 1)

level	# elem.	$\|\mu - \mu_h^d\|_h$	$\|\mu - \mu_h^q\|_h$	$\|\mu - \mu_h^b\|_h$	$\|\mu - \mu_h^c\|_h$
0	28	9.470143e-03	9.731379e-03	1.252511e-02	9.435581e-03
1	112	1.620246e-03	1.674903e-03	2.265275e-03	1.604492e-03
2	448	2.767632e-04	2.880399e-04	4.077914e-04	2.728400e-04
3	1792	4.787615e-05	5.007306e-05	7.302227e-05	4.707297e-05
4	7168	8.362299e-06	8.771935e-06	1.300681e-05	8.210304e-06
5	28672	1.468960e-06	1.543415e-06	2.308726e-06	1.441193e-06
6	114688	2.588398e-07	2.721896e-07	4.089964e-07	2.538517e-07

Table 2: Discretization errors in the weighted Lagrange multiplier norm, (Example 2)

level	# elem.	$\|\mu - \mu_h^d\|_h$	$\|\mu - \mu_h^q\|_h$	$\|\mu - \mu_h^b\|_h$	$\|\mu - \mu_h^c\|_h$
0	20	2.393161e+00	2.515256e+00	3.143823e+00	2.492000e+00
1	80	8.601690e-01	9.046823e-01	1.309716e+00	8.742536e-01
2	320	1.680722e-01	1.488028e-01	2.678213e-01	1.622111e-01
3	1280	2.113279e-02	2.279722e-02	3.357682e-02	2.199264e-02
4	5120	3.480169e-03	3.699532e-03	5.332353e-03	3.548563e-03
5	20480	5.915244e-04	6.262941e-04	8.860717e-04	6.020646e-04
6	81920	1.034967e-04	1.094254e-04	1.542287e-04	1.051368e-04

Table 3: Discretization errors in the weighted Lagrange multiplier norm, (Example 3)

level	# elem.	$\|\mu - \mu_h^d\|_h$	$\|\mu - \mu_h^q\|_h$	$\|\mu - \mu_h^b\|_h$	$\|\mu - \mu_h^c\|_h$
0	47	3.435663e-02	3.472259e-02	3.746504e-02	3.457403e-02
1	188	6.794099e-03	7.249089e-03	1.011761e-02	7.118611e-03
2	752	1.031815e-03	1.094674e-03	1.515990e-03	1.068923e-03
3	3008	1.829821e-04	1.968839e-04	2.880542e-04	1.904619e-04
4	12032	3.198112e-05	3.459908e-05	5.179677e-05	3.335310e-05
5	48128	5.642177e-06	6.117301e-06	9.213434e-06	5.887483e-06
6	192512	9.928575e-07	1.076081e-06	1.628637e-06	1.034036e-06

In all our examples the difference in the errors for the different Lagrange multiplier spaces in the L^2- and in the H^1-norm can be neglected. Only in the weighted Lagrange multiplier norm, we observe some quantitative difference. However, the qualitative results are the same. We note that better results can be obtained if Lagrange multiplier basis functions are used having a small maximum value. The Lagrange multiplier spaces M_h^d and M_h^c yield better results than the space M_h^b. In contrast to the discretization error in the L^2-norm and in the H^1-norm, the weighted L^2-norm for the Lagrange multiplier is very sensitive to the choice of the Lagrange multiplier space. It turns out that the quality of the Lagrange multiplier space depends on the maximum value of its nodal basis functions.

In our last example, we consider a decomposition of $\Omega = (0,1) \times (0,1)$ into four subdomains defined by $\Omega_{ij} := ((i-1)/2, i/2) \times ((j-1)/2, j/2), 1 \leq i \leq 2, 1 \leq j \leq 2$, with non-matching triangulations at the interfaces. For this example, we use

$$-\mathrm{div}(a\nabla u) + u = f \quad \text{in} \quad \Omega,$$

and we choose a to be 1 in Ω_{11} and Ω_{22}, and $a = 3$ in Ω_{21} and Ω_{12}. Figure 16 shows the decomposition into four subdomains, our initial non-matching triangulation and the isolines

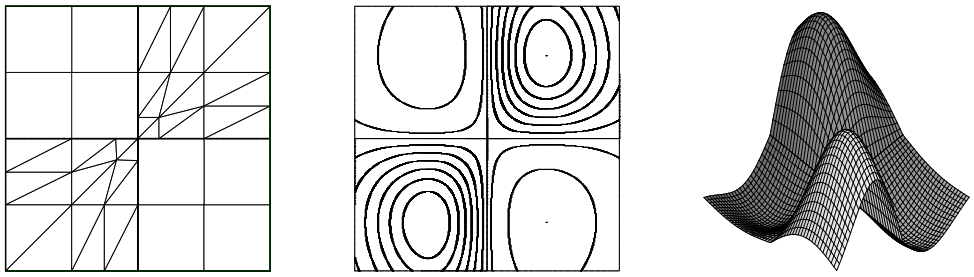

Figure 16: Decomposition into four subdomains and initial triangulation (left), isolines of the solution (middle) and exact solution (right), (Example 4)

of the solution. Here, we choose the exact solution $u(x,y) = (x-1/2)(y-1/2)\exp(-10\,(x-1/2)^2 - 5\,(y-1/2)^2)/a$, see Figure 16.

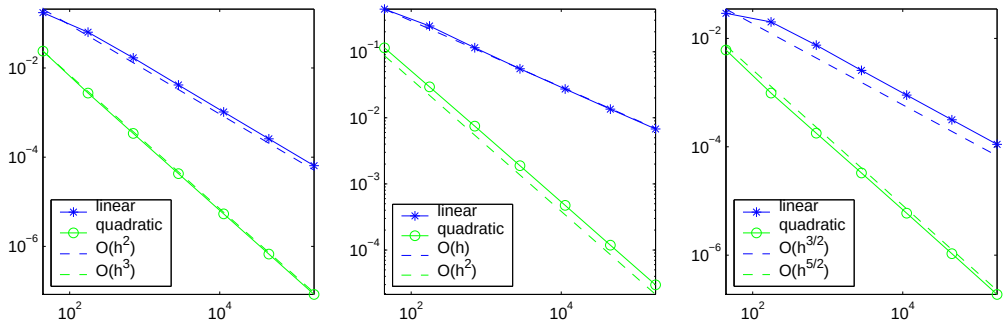

Figure 17: Error plot versus number of elements, L^2-norm (left), H^1-norm (middle), weighted Lagrange multiplier norm (right), (Example 4)

The discretization errors are shown in Figure 17. The solution has a jump in the normal derivative at the interface but not in the flux.

References

[BBJ+97] P. Bastian, K. Birken, K. Johannsen, S. Lang, N. Neuß, H. Rentz–Reichert, and C. Wieners. UG – a flexible software toolbox for solving partial differential equations. *Computing and Visualization in Science*, 1:27–40, 1997.

[BD98] D. Braess and W. Dahmen. Stability estimates of the mortar finite element method for 3–dimensional problems. *East–West J. Numer. Math.*, 6:249–263, 1998.

[Bel99] F. Ben Belgacem. The mortar finite element method with Lagrange multipliers. *Numer. Math.*, 84:173–197, 1999.

[BHS01] R. Becker, P. Hansbo, and R. Stenberg. A finite element method for domain decomposition with non-matching grids. *Preprint 2001-15, Chalmers University of Technology, Goetborg, Sweden*, 2001. to appear in M^2AN.

[BM97] F. Ben Belgacem and Y. Maday. The mortar element method for three dimensional finite elements. *M^2AN*, 31:289–302, 1997.

[BMP93] C. Bernardi, Y. Maday, and A.T. Patera. Domain decomposition by the mortar element method. In H. Kaper et al., editor, *Asymptotic and numerical methods for partial differential equations with critical parameters*, pages 269–286. Reidel, Dordrecht, 1993.

[BMP94] C. Bernardi, Y. Maday, and A.T. Patera. A new nonconforming approach to domain decomposition: the mortar element method. In H. Brezzi et al., editor, *In: Nonlinear partial differential equations and their applications*, pages 13–51. Paris, 1994.

[HN01] B. Heinrich and S. Nicaise. Nitsche mortar finite element method for transmission problems with singularities. *Preprint 2001-10, TU Chemnitz*, 2001.

[KLPV01] C. Kim, R.D. Lazarov, J.E. Pasciak, and P.S. Vassilevski. Multiplier spaces for the mortar finite element method in three dimensions. *SIAM J. Numer. Anal.*, 39(2):519–538, 2001.

[OW01] P. Oswald and B.I. Wohlmuth. On polynomial reproduction of dual FE bases. In N. Debit, M. Garbey, R. Hoppe, J. Pèriaux, D. Keyes, and Y. Kuznetsov, editors, *Thirteenth International Conference on Domain Decomposition Methods*, pages 85–96, 2001.

[SS98] P. Seshaiyer and M. Suri. Convergence results for non-conforming hp methods: The mortar finite element method. *Contemporary Mathematics*, 218:467–473, 1998.

[SS00] P. Seshaiyer and M. Suri. Uniform hp convergence results for the mortar finite element method. *Mathematics of Computations*, 69:521–546, 2000.

[Ste98] R. Stenberg. Mortaring by a method of J.A. Nitsche. In S. Idelsohn, E. Onate, and E. Dvorkin, editors, *Computational Mechanics: New Trends and Applications*, Barcelona, 1998. CIMNE.

[Woh00] B.I. Wohlmuth. A mortar finite element method using dual spaces for the Lagrange multiplier. *SIAM J. Numer. Anal.*, 38:989–1012, 2000.

[Woh01] B.I. Wohlmuth. *Discretization Methods and Iterative Solvers Based on Domain Decomposition*, volume 17 of *LNCS*. Springer Heidelberg, 2001.

[Woh02] B.I. Wohlmuth. A comparison of dual Lagrange multiplier spaces for mortar finite element discretizations. *Preprint 2001-17, University of Stuttgart*, 2002. to appear in *M^2AN*.